BEER – The Beamline for European Materials Engineering Research at the ESS

J Fenske[1], M Rouijaa[1], J Šaroun[2], R Kampmann[1], P Staron[1], G Nowak[1], J Pilch[2,3], P Beran[2], P Šittner[3], P Strunz[2], H-G Brokmeier[4], V Ryukhtin[2], L Kadeřávek[2,3], M Strobl[5,6], M Müller[1], P Lukáš[2] and A Schreyer[1]

[1] Helmholtz-Zentrum Geesthacht, Max-Planck-Str. 1, 21502 Geesthacht, Germany
[2] Nuclear Physics Institute, ASCR, Hlavní 130, 25068 Řež, Czech Republic
[3] Institute of Physics, ASCR, Na Slovance 2, 18221 Praha 8, Czech Republic
[4] Clausthal University of Technology, Adolph Roemer-Straße 2a, 38678 Clausthal-Zellerfeld, Germany
[5] European Spallation Source, Tunavägen 24, SE-22100 Lund, Sweden
[6] University of Copenhagen, Niels Bohr Institute, Universitetsparken 5, 2100 Copenhagen, Denmark.

E-mail: jochen.fenske@hzg.de

Abstract. The Beamline for European Materials Engineering Research (BEER) will be built at the European Spallation Source (ESS). The diffractometer utilizes the high brilliance of the long-pulse neutron source and offers high instrument flexibility. It includes a novel chopper technique that extracts several short pulses out of the long pulse, leading to substantial intensity gain of up to an order of magnitude compared to pulse shaping methods for materials with high crystal symmetry. This intensity gain is achieved without compromising resolution. Materials of lower crystal symmetry or multi-phase materials will be investigated by additional pulse shaping methods. The different chopper set-ups and advanced beam extracting techniques offer an extremely broad intensity/resolution range. Furthermore, BEER offers an option of simultaneous SANS or imaging measurements without compromising diffraction investigations. This flexibility opens up new possibilities for in-situ experiments studying materials processing and performance under operation conditions. To fulfil this task, advanced sample environments, dedicated to thermo-mechanical processing, are foreseen.

1. Introduction

Engineering materials will have paramount importance for the technological progress of mankind in the coming decades. There is presently a transition towards more complex multi-phase and/or composite materials with specially designed microstructures and tailored functional properties for particular purposes of usage. Examples of such materials are high temperature and corrosion resistant intermetallics for gas turbines, lightweight materials for transport applications or multi-functional coatings in industrial gas turbines. These novel materials, together with modern material production technologies, are urgently needed to tackle societal challenges related to sustainable development, particularly future means of transportation and mobility, energy production, distribution and storage as well as medical devices for health care and smart structures for civil engineering.

Progress in development, fabrication, optimization, and degradation monitoring of modern engineering materials is essential for the production of more efficient, more environmentally friendly and more durable engineering components. To achieve such ambitious goals, employment of science-based approaches towards material design and development as well as adoption of new methods for production, thermomechanical processing, testing and characterization of materials is required [1].

Neutron diffraction is a well-established tool for characterization of engineering materials [2,3] and components, e.g. for analysis of internal stresses and textures [4,5] or phase analysis [6]. The strength of neutron scattering, however, lies especially in in-situ investigations of advanced materials in complex sample environments [7]. Particularly for material engineering research, it will be extremely helpful to replicate real fabrication, processing and in-operando conditions in neutron beams. It will move analytical processing and performance research from post mortem analysis to yet unparalleled in-situ or in-operando analysis. Such research will lead to breakthroughs in optimization of various engineering materials processing, e.g. development of advanced methods of joining such as friction stir welding or improvements of industrial processing such as casting, hot rolling, forging and annealing. Therefore academic as well as industrial users will benefit from new in-situ and in-operando neutron diffraction experiments.

The unique concept of BEER (**B**eamline for **E**uropean Materials **E**ngineering **R**esearch) was developed to offer these possibilities. The diffractometer is based on a significant improvement in data acquisition times compared to current materials engineering flagship instruments, a flexible detector coverage, additional small-angle scattering (SANS) and imaging options and complex sample environments. The concept is mainly driven by:

(I) enabling time-resolved in-situ and in-operando investigations of structural materials during processing and exposure to simulated service environments,

(II) adopting state-of-the-art technologies for efficient and precise characterization of residual stresses, crystallographic textures and phase compositions in structural materials.

Thus, new opportunities will be offered to material engineers for studying the evolution of micro and nanostructures, phase transformations, textures and internal stresses at industrially relevant temperatures, strain rates and complex loading conditions. This will help to investigate and develop thermomechanical processing procedures as well as to study fatigue mechanisms under service conditions.

2. General Instrument Layout

BEER will be a 159 m long time-of-flight (ToF) diffractometer supplemented by a detector for optional SANS measurements. Figure 1 shows the instrument layout with the basic components: a bi-spectral extraction system inside the target monolith, a cave after the monolith with choppers for pulse shaping (PSC), frame definition (FC) and modulation (MC), followed by expanding and curved guide sections, a divergence slit, an exchangeable focusing guide and a sample stage surrounded by detectors. These components and their functions are described in the following sections.

The neutron optics design and performance parameters presented here are based on the ESS moderator concept of 2013 [8]. Since then, the neutron optics concept has been under further development to match the newly proposed low-dimensional moderators [9]. Although this modification does not affect the overall concept, some of the parameters are affected [10].

2.1. Source and bi-spectral extraction optics

The neutron optics system has to collect neutrons from both the thermal and cold moderators with an active area of 120×120 mm^2, arranged side by side with a 10 mm gap, according to the ESS moderator concept of 2013 [8]. The proposed bi-spectral extraction method follows the study by Zendler et al. [11]. It consists of an array of 7 semi-transparent mirrors on 0.5 mm thick Si substrate with a length of 0.5 m, which transmit thermal neutrons from the thermal moderator and reflect low-energy neutrons from the cold moderator into the same guide. The supermirror coating with m=4.7 (m=1 corresponds

to the critical angle of Ni, 0.1°/Å) and the inclination angle of 0.95° matches the crossover wavelength of 2.0 Å between the cold and thermal spectra. The distance of the extraction system from the source of 3.7 m and the mirrors length of 0.5 m result from the beam size and source geometry. Further optimization by Monte Carlo simulations indicated an improvement of transmittance if this mirror array is slightly convergent with an angle of about ~0.75°.

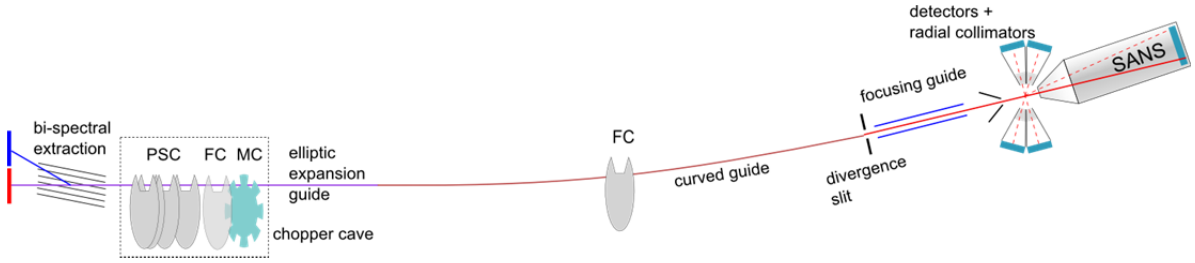

Figure 1: Schematic drawing of the BEER layout with the key components, e.g. pulse shaping (PSC), frame definition (FC) and modulation choppers (MC): for details see the text.

2.2. Neutron transport

The neutron transport optics is 157 m long and starts at 2 m behind the source with a 4 m long monolith insert including the bi-spectral extraction optics and a pair of vertically reflecting mirrors. It serves as a feeder for a narrow parallel guide (20×80 mm^2) in the chopper section, which is 3.5 m long and is interrupted by several gaps for the choppers. This section is followed by a 15 m long guide expanding elliptically from the width of 20 mm to 40 mm; the height of 80 mm is conserved. A consecutive parallel, horizontally curved guide with a length of 129 m, a cross section of 40×80 mm² and a radius of curvature of 20 km blocks the direct line of sight at about 85 m from the source, which helps to reduce radiation background in the experimental area. An adjustable slit for tuning the beam divergence marks the end of the long guide. It is followed by an optional 5.5 m long focusing guide that is elliptically tapered in vertical direction and parallel in horizontal direction. This focusing guide ends 1 m before the sample leaving enough space for large sample environments. The guide is divided in two sub-sections with lengths of 3.5 m and 2 m, which are removable and can be optionally replaced by slits or a horizontally focusing multichannel segment. These options allow for adjustment of the beam divergence in a wide range and, together with variable chopper settings, to efficiently trade resolution for intensity as required by the variety of experiments to be carried out at BEER. The neutron optics concept is described in more details in [10].

2.3. Pulse-shaping choppers

Pulse-shaping choppers (PSC) close to the source are required to tune the $\Delta\lambda/\lambda$ resolution in a range suitable for diffraction. Four such choppers will be installed in the cavity after the monolith, with the first chopper at a minimum practically feasible distance of 6.45 m (the basic chopper parameters are listed in table 1). This minimum distance together with the ESS pulse length of τ=2.86 ms and the repetition rate of 14 Hz basically restricts the bandwidth to $\Delta\lambda$<1.73 Å. The path length which optimally fills the interval between subsequent ESS pulses at the detector (T=71.4 ms) is L_D=163 m. Two PSC's are operated at the same time in optically blind mode, i.e. the second disk opens when the first disk closes. This technique has been introduced by van Well [12] and is nowadays a common technique used at various neutron instruments. The main advantage of this concept is that the wavelength resolution ($\Delta\lambda/\lambda$) does not depend on the wavelength, which permits more efficient use of the source flux by using longer opening times for longer wavelengths. The different distances between the choppers (150 – 1200 mm) and combinations of the four choppers allow for a $\Delta\lambda/\lambda$ resolution between 0.1 and 0.8 %.

Table 1: Basic parameters of the choppers for pulse shaping (PSC), beam modulation (MC) and frame definition (FC).

ID	distance [m]	frequency [Hz]	beam width/height [mm]	window width [deg]
		Pulse Shaping		
PSC1	6.45	168	20/80	144
PSC2	6.6	168	20/80	144
PSC3	6.9	168	20/80	144
PSC4	7.65	168	20/80	144
		Modulation		
MCa	8.95	42 … 280	20/80	16 × 4°, distance 22.5°
MCb	9.00	42 … 280	20/80	4 × 4°, distance 90°
MCc	9.50	42 … 70	20/80	1 × 180°, followed by 7 × 4°, distance 22.5°
		Frame Definition		
FC1a	8.28	14/7	20/80	70
FC1b	8.32	63/70	20/80	180
FC2a	79.55	14	40/80	180
FC2b	79.59	7	40/80	90

2.4. Frame definition choppers

There are two double disc choppers available for wavelength frame definition, FC1 and FC2, located at 8 m and 80 m from the source, respectively. Further details are listed in table 1. They permit to define either the standard bandwidth of $\Delta\lambda\approx1.7$ Å, as given by the source pulse length of 2.86 ms and the PSC distance, or an extended bandwidth. The latter can be achieved by two methods. The first one consists in the suppression of one or more subsequent pulses and tuning FC2 so that it selects a quasi-continuous wavelength band of the width $\Delta\lambda\approx n\times1.7$ Å. This mode can only be used in combination with the pulse multiplexing technique described in the following section, since the pulse shaping system does not allow for sufficient suppression of frame overlaps. The second method is the so-called alternating wavelength frame mode. In this case, the FC choppers are set in such a way that alternately either thermal or cold neutrons arrive at the detectors at subsequent time frames. In this case, the two wavelength frames are separated by the gap $\Delta\lambda_s=1.77$ Å.

2.5. Modulation choppers

For the modulation techniques three different choppers are alternatively available MCa, MCb and MCc located at a distance between 8.95 and 9.5 m from the source (the basic parameters of the MCs are listed in table 1). The choppers are operated together with the frame definition choppers FC1 and FC2 for setting the wavelength frame while the pulse shaping choppers PSC are stopped. The pulse modulation technique works as follows: Seen from one moment in time from the detector the ESS source pulse of 2.86 ms creates at the modulation chopper position at about 9 m from the moderator a virtual source with a pulse length of 2.70 ms. The MC's modulate this virtual source into a chain of sub-pulses with a pulse-to-pulse interval Δt_{ptp} depending on the frequency and the slit distance of the MC's. The number of sub-pulses is given by $M_d=2.70\text{ms}/\Delta t_{ptp}$. M_d is called hereafter as multiplexing degree. At the highest frequency of 280 Hz, up to 12 sub-pulses are formed by the MCa chopper. Thus, several neutron pulses arrive at the detectors at the same time, which are well distinguished in wavelength. At a lower frequency less sub-pulses are formed (e.g. $M_d=3.5$ for $f=70$ Hz). The pulse modulation results in a multiplexing of Bragg reflections as shown in figure 2 for a frequency of 210 Hz. Thus, the pulse modulation technique leads to a gain in intensity of 2–12 (corresponding to the multiplexing degree M_d) without relaxing the Q-resolution. This operation mode gives a huge advantage, e.g. for increasing the time resolution of in-situ experiments or reducing counting times for mapping of residual strains. The distance between split sub-peaks can be increased while keeping the resolution, if for example the peak tails shall be analyzed, by using the MCb chopper instead of MCa. Here, the larger distance between the slits leads to a larger distance between the sub-peaks.

If the pulse distance is larger than the length of the virtual source, M_d becomes <1 which means that at any moment in time neutrons of only one wavelength arrive at the detector, referred to in the following as "one-λ-mode". This is the case if MCb runs with a frequency below ≤98 Hz.

The pulse modulation technique and the one-λ-mode can be combined with the pulse suppression technique to extend the bandwidth, e.g. for capturing texture changes in in-situ experiments where the sample cannot be rotated. The unique design of MCc in combination with the alternating wavelength frame mode allows for the modulation of thermal neutrons while neutrons from the cold wavelength range pass the chopper unhindered giving an opportunity to combine diffraction and SANS measurements.

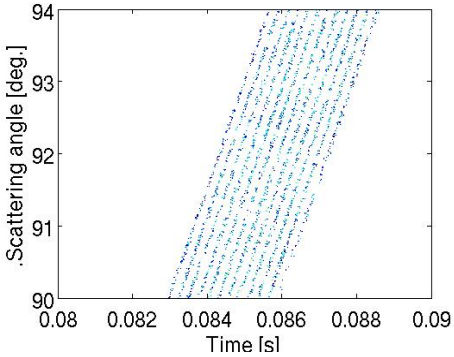

Figure 2: Examples of a multiplexed Bragg reflection (Al powder, (220)) as simulated by means of McStas [13] with a MCa frequency of 210 Hz.

2.6. Detectors

The variety of complex sample environments foreseen at the BEER instrument requires a flexible system of detectors allowing for both angular and time analysis of diffraction data. The arrangement of detectors and their distances have to allow for large in-situ devices such as the GLEEBLE® system [14] to be installed at the sample. Therefore the detectors are placed at a distance of 2 m from the sample position. The proposed detector arrangement leaves the necessary space along the axis of deformation devices. Four main detectors (D1–D4), each covering about 30×30 deg^2 (area 1 m^2) are positioned as shown in figure 3. The detectors are mounted together with attached radial collimators on rails, which permit precise radial movement and opening of the experimental space during installation of a large sample environment. A smaller detector at a shorter distance (~1.5 m) with medium spatial resolution (~5×5 mm^2) placed at one side of the incident beam allows for measurements in backscattering geometry, offering high resolution data especially for structural refinement. In the transmitted beam, a small (~40×40 mm^2) high-resolution (app. 100 µm) position-sensitive detector serves for imaging studies, with the possibility of energy analysis, i.e. Bragg edge imaging. Alternatively a 1×1 m^2 detector for SANS measurements is available in a vacuum tank at up to 6.5 m behind the sample. This maximum distance is determined by the distance of the divergence slit in front of the sample, which will be used for both diffraction and SANS.

An additional arc detector bank in the plane perpendicular to the incident beam enables sufficient angular coverage for texture and strain analyses. This detector arc will have a shorter distance (≈1 m) from the sample to optimise its active area for required angular coverage (e.g. 3 segments, 0.6×0.5 m^2 each, covering together an arc of about 100°×30°).

2.7. Sample environments

BEER will be equipped with dedicated sample environments for in-situ measurements of different kinds, covering both fast and slow processes. This includes devices for in-situ physical simulation of materials processing such as the GLEEBLE® simulator [14] or a quenching and deformation dilatometer [15]. A midsize deformation rig is foreseen for in-situ material testing as well as a small-size deformation rig positioned with a goniometer or a robot. Additionally, deformation rigs for long-term material testing and shared standard sample environments e.g. cryostats, magnets, furnaces will be used. The beamline layout allows for horizontal access to the sample area and for installation of user supplied sample environments. The main positioning table with a load capacity of 3 tons, rotation

range ±360°, and vertical movement is required for precise positioning of sample environments. Several other standard positioning systems (hexapod, precise xyz stage, goniometer, robot, etc.) can be mounted on the main positioning table and will ensure a secondary precision movement of the sample or smaller sample environments.

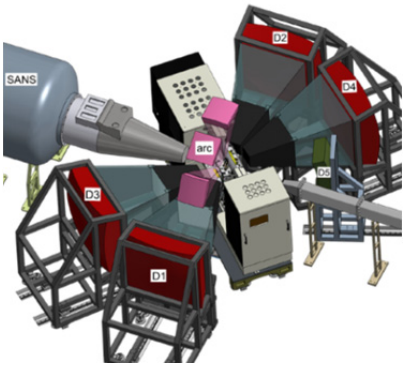

Figure 3: View of the sample area with proposed detector banks. Detectors can be retracted for bringing in large sample environment, e.g. as shown the GLEEBLE® simulator [14]. In the horizontal plane, the detectors are centred at 2θ=90° (D1), -90° (D2), 50° (D3), -130° (D4) and -160° (D5). In addition, an arc of detectors spans about 100° in the plane normal to the incident beam, filing partly the gap between the detectors D1 and D2. This arc is required mainly for texture analysis.

3. Performance

BEER offers a broad range of operation modes, e.g. pulse shaping or modulation. The neutron fluxes and resolutions for the various operation modes were obtained by Monte Carlo simulations assuming the moderator brightness baseline of 2013 [8]. The results are summarized in figure 3 together with similar data available for world leading ToF engineering diffractometers. For the ESS data, resolutions were evaluated from the peak widths of the Fe (211) and Fe (110) diffraction lines simulated for the detector bank at 2θ=75°…105°. For the other instruments, simulated data is shown when available (ENGIN-X [16], VULCAN at cold λ-range) or the data from the instruments web pages (TAKUMI [17], IMAT [18], VULCAN at thermal λ-range [19–21]). It should be underlined that these integrated intensities do not allow for direct calculation of count rates at a given diffraction line and the simulations do not include some aspects of physical reality such as absorption in Al windows or air scattering. Moreover, the flux values for the other instruments correspond to different wavelength intervals because of the different lengths and source frequencies. In spite of this, figure 3 clearly shows the excellent performance of BEER in terms of flexibility in trading resolution for high flux. The combination of variable $\Delta\lambda/\lambda$ resolutions and focusing optics allows for a significantly wider range of choices concerning tailoring flux and resolution to the needs of specific measurements as compared to the existing instruments at short-pulse sources. In addition, the pulse modulation method can preserve high flux at high resolutions, provided that the crystal structure allows for evaluation of the multiplexed diffraction lines.

The simulations show that the expected high flux enables very fast measurements. Counting times shorter than 1 s can be reached in the high flux (HF) and pulse modulation (MLR) modes with focusing optics. Even single pulse measurements (sampling at 14 Hz) seem to be possible for specific samples and studies, e.g. in-situ hot-compression tests on 2Mn-0.2C steel rods with a diameter of 7 mm using the medium resolution mode (MR).

The performance of BEER allows for residual stress investigations and for texture measurements. The detector arrangement provides the opportunity to measure a complete pole figure by the rotation of the sample around just the tension axis.

Furthermore, BEER offers the opportunity to combine diffraction measurements with SANS or imaging without a penalty for the diffraction performance. The slit at a distance of L=6.5 m from the sample for tuning the beam divergence for diffraction can also be used to define an aperture for imaging. Its size, D is continuously adjustable, allowing thus for imaging measurements with the L/D collimation ratio ranging from 115 to more than 1000. Although the imaging characteristics are in general worse when compared to ODIN [22,23] the proposed dedicated imaging instrument at ESS, they become complementary for high energy resolution. For $\Delta\lambda/\lambda$ ~0.3% (at λ=2.0…3.7 Å) and an L/D ratio of 504 the simulated flux is about $3.4\cdot10^6$ n/s/cm^2. The corresponding flux per wavelength interval (flux density) is about a factor 2.6 higher than at ODIN and allows for sub-second exposure

times. The tuneable wavelength resolution is suitable for energy resolved imaging, i.e. Bragg edge analysis, and hence mapping of various microstructural characteristics, e.g. phase composition, texture and strains [24,25].

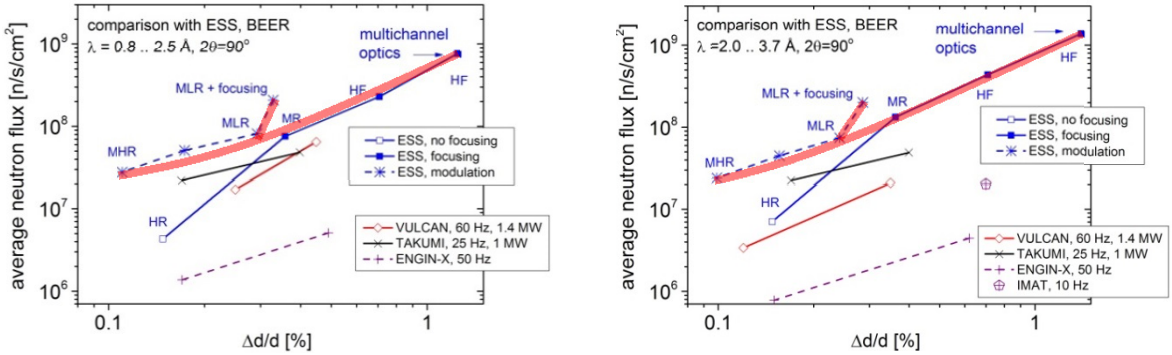

Figure 3: Simulated time-averaged flux at the sample as function of resolution for different operation modes (Pulse modulation with high resolution (MHR) ($\Delta\lambda/\lambda$=0.07%, divergence slit: 10×80 mm²), pulse modulation with low resolution (MLR) (0.27%, 40×80 mm²), high resolution (HR) (0.1%, 15×80 mm²), medium resolution (MR) (0.3%, 40×80 mm²) and high flux (HF) (0.8%, 40×80 mm²)) of BEER at thermal (left side) and cold (right side) wavelength ranges. The values for the modulation mode were simulated without focusing, except of the last point as indicated. Data available for VULCAN (SNS), TAKUMI (MLF), ENGIN-X and IMAT (both ISIS) are shown for comparison.

Like for imaging, the divergence aperture can be used to increase the resolution for simultaneous diffraction and SANS measurements. Its position determines the optimum SANS detector distance to be about 6.5 m. The alternating frame technique has to be used to define thermal and cold neutron wavelength bands in subsequent pulses in order to carry out simultaneous SANS and diffraction measurements with pulse shaping choppers. Positions of these bands can be varied synchronously by changing the chopper phases in order to extend the Q-range. Table 2 gives an example of conditions under which the simultaneous SANS and diffraction measurement are feasible. The calculation assumes a medium resolution diffraction mode with the divergence slit size of 40×40 mm^2 and $\Delta\lambda/\lambda$=0.3%. Although the SANS characteristics are worse when compared to proposed dedicated instruments at the ESS, e.g. SKADI [26], they are still significantly better than e.g. for the well established V4 instrument at HZB [27] (flux ~4.6·10^6 n/s/cm^2 for λ=5 Å, $\Delta\lambda/\lambda$=10%, collimation and detector distances L=2 m, divergence slit 30×50 mm^2). It can thus be concluded that extremely important information about kinetics of formation of pores and precipitates can be obtained by the combination of diffraction measurements with SANS without compromising diffraction investigations.

Table 2: Examples of estimated SANS and diffraction characteristics in the case of simultaneous SANS and diffraction measurements.

	flux	wavelength	resolution	d-range
diffraction	9.6·10^6 [n/s/cm²]	1.2 … 2.9 Å	Δd/d ~ 0.4 %	0.7 ... 2.3 Å
SANS	6.2·10^6 [n/s/cm²]	4.7 … 6.3 Å	δQ ~ 0.003 Å^{-1}	20 … 350 Å

4. Summary

BEER will be a unique instrument that offers a broad range of operation modes, spanning over one decade in resolution. The simulations predict a neutron flux approaching 10^9 n/cm^2/s which unlocks an unparalleled potential for fast kinetic experiments with sub-second time resolution. Under favourable circumstances, e.g. strong scattering and suitable sample volume, measurements with a single pulse, i.e. a 14 Hz sampling rate, should be feasible. In addition, the novel pulse modulation technique permits to preserve high flux also at high resolution in the case of materials with high symmetry, i.e. with well-separated diffraction lines. The possibility of simultaneous diffraction and SANS or imaging measurements without penalty for the diffraction performance strengthens the ability of the instrument to address growing interest in microstructure characterization during material processing. BEER will

also provide a large experimental area at the sample position, allowing for unique in-situ experiments with large high-power sample environment devices required for such studies.

Acknowledgments
This work has been supported by the BMBF under the contract number 05E11G1 within the German contribution to the Design-Update project of the European Spallation Source. Preparation of the instrument project was further supported by the Czech Ministry of Education, Youth and Sports under the project LM 2010011.

References

[1] Jarvis D 2012 *Metallurgy Europe - A Rennaissance Programme for 2012-2022* (Strasbourg) <http://www.esf.org/fileadmin/Public_documents/Publications/metallurgy_europe.pdf>
[2] Wang X L 2006 *JOM* **58** 52
[3] Reimers W, Pyzalla A, Schreyer A and Clemens H 2008 *Neutron and Synchrotron Radiation in Engineering Materials Science* (Weinheim: Wiley-VCH)
[4] Krawitz A D 2001 *Introduction to diffraction in material science and engineering* (New York: Wiley)
[5] Brokmeier H-G and Yi S B 2008 *Neutron and Synchrotron Radiation in Engineering Materials Science,* ed W Reimers, A Pyzalla, A Schreyer and H Clemens (Weinheim: Wiley-VCH) pp 57-77
[6] Billinge S J L 2006 *JOM* **58** 47
[7] Kannengiesser T, Babu S S, Komizo Y and Ramirez A J 2010 *In situ Studies with Photons, Neutrons and Electrons Scattering* (Berlin Heidelberg: Springer)
[8] Peggs S 2013 *ESS Technical Design Report* (Lund) <http://eval.esss.lu.se/cgi-bin/public/DocDB/ShowDocument?docid=274> 2015-10-07
[9] Ferenc Mezei F, Zanini L, Takibayev A, Batkov K, Klinkby E B, Pitcher E and Schönfeldt T 2014 *Journal of Neutron Research* **17** 101
[10] Šaroun J, Fenske J, Rouijaa M, Beran P, Navrátil J, Lukáš P, Schreyer A and Strobl M *Neutron optics concept for the materials engineering diffractometer at the ESS,* this issue
[11] Zendler C, Lieutnant K, Nekrassov D, Cussen L D and Strobl M 2013 *Nucl. Inst. Meth.* A **704** 68
[12] van Well A A 1992 *Physica* B **180–181** 959
[13] Willendrup P, Farhi E and Lefmann K 2004 *Physica* B **350** 735
[14] <gleeble.com> 2015-10-07
[15] Staron P et al. 2011 *Advanced Engineering Materials* **13** 658
[16] private communication with Shu Yan Zhang 2015-10-01
[17] <http://j-parc.jp/researcher/MatLife/en/instrumentation/ns_spec.html#bl19> 2015-10-07
[18] Kockelman W, Zhang S Y, Kelleher J F, Nightingale J B, Burca G and James J A 2013 *Physics Procedia* **43**, 100
[19] <http://neutrons.ornl.gov/sites/default/files/Instrument_7.pdf> 2015-10-07
[20] An K, Skorpenske H D, Stoica A D, Ma D, Wang X L and Cakmak E 2011 *Metallurgical and Materials Transactions* A **42** 95
[21] Wang X L, Holden T M, Stoica A D, An K, Skorpenske H D, Jones A B, Rennich G Q and Iverson E B 2010 *Mater. Sci. Forum* **652** 105
[22] <https://europeanspallationsource.se/sites/default/files/odin_imaging_instrument_construction_proposal.pdf> 2015-10-07
[23] Strobl M 2015 *Physics Procedia* **69** 18-26
[24] Santisteban J R, Edwards L, Steuwer A and Withers P J 2001 *J. Appl. Cryst.* **34** 289
[25] Strobl M 2009 *Nucl. Instr. and Meth.* A **604** 646–652
[26] <https://europeanspallationsource.se/sites/default/files/skadi_proposal.pdf> 2015-10-07
[27] <https://www.helmholtz-berlin.de/pubbin/igama_output?modus=einzel&sprache=en&gid=1706&typoid=39942> 2015-10-07